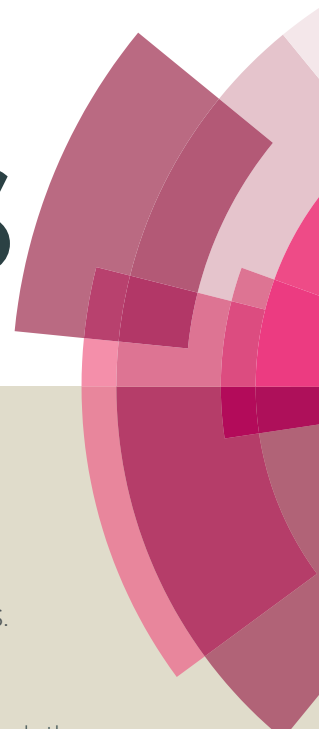


# RSC Advances



This article can be cited before page numbers have been issued, to do this please use: S. P. Anthony, S. Nagarajan, M. S. Muthuraman, V. K. Vadivel, L. R. Christena and P. Praveen, *RSC Adv.*, 2016, DOI: 10.1039/C6RA06806E.



This is an *Accepted Manuscript*, which has been through the Royal Society of Chemistry peer review process and has been accepted for publication.

*Accepted Manuscripts* are published online shortly after acceptance, before technical editing, formatting and proof reading. Using this free service, authors can make their results available to the community, in citable form, before we publish the edited article. This *Accepted Manuscript* will be replaced by the edited, formatted and paginated article as soon as this is available.

You can find more information about *Accepted Manuscripts* in the [Information for Authors](#).

Please note that technical editing may introduce minor changes to the text and/or graphics, which may alter content. The journal's standard [Terms & Conditions](#) and the [Ethical guidelines](#) still apply. In no event shall the Royal Society of Chemistry be held responsible for any errors or omissions in this *Accepted Manuscript* or any consequences arising from the use of any information it contains.



Journal Name

ARTICLE

## L-Methionine Based Phenolic Compound Mediate Unusual Assembly of AgNPs and Exert Efficient anti-biofilm effect

V. Vinod Kumar,<sup>a</sup> Lawrence Rene Christena,<sup>b</sup> P. Praveen,<sup>a</sup> Meenakshi Sundaram Muthuraman,<sup>b</sup> Nagarajan Saisubramanian<sup>b\*</sup> and Savarimuthu Philip Anthony<sup>a\*</sup>

Received 00th January 20xx,  
Accepted 00th January 20xx

DOI: 10.1039/x0xx00000x

www.rsc.org/

2-(2-hydroxybenzylamino)-4-(methylthio)butanoic acid (L) together with capping molecules, produced AgNPs with unusual nanostructures that showed efficient inhibition of biofilm growth. Nanoplates of AgNPs self-assemble into micron sized flower-petal like structures in L-PSS-AgNPs whereas mesocrystals with visible voids from smaller nanoplates has formed in L-SDS-AgNPs. L-PVA- and L-PVP-AgNPs showed polydispersed multi-shaped nanoparticles including nanoprisms, spheres and plates. The structure-property studies indicate that slow reduction of Ag<sup>+</sup> ions and thiophilic interaction of L is responsible for unusual morphology and organization of AgNPs. Importantly L-capping molecules-AgNPs exhibited strong biofilm inhibitory effect against four different bacteria, *S. aureus*, *P. aeruginosa*, *B. subtilis* and *E. coli* of which, the former two are classical colonizers in burn wounds. BIC (Biofilm inhibitory concentration) and MIC (Minimum inhibitory concentration) studies further confirmed the true anti-biofilm effect AgNPs. Studies to unravel the mechanism of action indicated that enhanced anti-biofilm effect could be attributed to altered membrane permeability and integrity caused by L, which in turn curtails bacterial colonization as revealed by confocal imaging. Thus a simple amino acid modified phenolic molecule exhibited interesting assembly of AgNPs with remarkable anti-biofilm activity, which holds promise for its potential use in fabrication of wound healing dressing materials.

### Introduction

Exploiting the unique physiochemical properties of metal nanoparticles for biological applications such as diagnostic and therapeutic studies have been the focus of material science in recent years.<sup>1-3</sup> Infectious diseases especially the ones caused by drug resistant pathogens pose a greater threat to public health worldwide and hence there is an urgent need to curtail it. Every year in US alone, more than 2 million people have been reported to be infected with drug resistant microbes, which accounts for at least 23000 deaths annually.<sup>4</sup> Since microbes resort to biofilm, instead of planktonic mode of growth, in many chronic infections and as biofilms, they display 100 to 1000 fold enhanced resistance to antimicrobial agents, of late intensive research effort has been made to develop effective anti-biofilm agents. Presence of nutrients and solid substratum are the prerequisites for biofilm formation by microbes. Most microbes easily attach to any solid substratum and resort to biofilm mode of growth.<sup>5-6</sup> Microbial cells in a biofilms are enmeshed within a complex and heterogeneous matrix known

as Extracellular Polymeric Substances (EPS) comprised of polysaccharides, peptides, protein and DNA that provides increased resistance against antimicrobial agents, disinfectants and the immune attack. Biofilms on chronic wounds/ medical devices serve as reservoirs for pathogens which results in persistent/recurrent infections. Hence the development of new biomaterials that could curtail biofilm formation on chronic wounds / on the surface of implantable medical devices is crucial.

The antimicrobial effect of silver (Ag) is known and has been used for years in the medical field for antimicrobial applications.<sup>7-9</sup> Silver nanoparticles (AgNPs) being one of the predominantly used nanoparticle is well known to display antimicrobial effect against a wide range of bacteria and fungi including drug resistant microbial strains due to its increased surface area.<sup>10</sup> AgNPs have been used for decades to treat burn wounds and to filter microorganisms from water.<sup>11</sup> The size, shape, atomic composition and surface ligands of AgNPs can modulate its antimicrobial activity.<sup>12-15</sup> More specifically, the surface ligand structure plays a significant role not only in controlling the morphology and providing the stability to NPs, but it also contributes towards augmenting the biological activity by promoting its adsorption or diffusivity into the bacterial membrane.<sup>16</sup> For example, AgNPs stabilized with cationic polymers lead to enhanced antibacterial effect due to the increased permeability.<sup>17</sup> Polymer capped AgNPs can be potentially employed as wound dressing material to prevent biofilm formation in infected wounds. A recent study has used AgNPs loaded silk fibroin/carboxy methyl chitosan

<sup>a</sup> Department of Chemistry, School of Chemical & Biotechnology, SASTRA University, Thanjavur-613401, Tamil Nadu, India. E-mail: philip@biotech.sastra.edu.

<sup>b</sup> Department of Biotechnology, School of Chemical & Biotechnology, SASTRA University, Thanjavur – 613401, Tamil Nadu, INDIA. E-mail: sai@sabt.sastra.edu. Electronic Supplementary Information (ESI) available: [Absorption spectra, HR-TEM images of AgNPs with different capping agents, antibiofilm effects of capping agent alone and confocal fluorescent microscopic images of antibacterial effect of AgNO<sub>3</sub>. See DOI: 10.1039/x0xx00000x

nanocomposite and proved that it exerted superior anti *Pseudomonas* effect relative to commercially available AQUACEL®; Ag, which could be attributed to improved moisture absorption, retention and water vapor transmission rate contributed by CMC.<sup>18</sup> Similarly PVP- carrageenan hydrogel impregnated with 100 ppm of AgNPs retained more fluid and released ~ 20 % of silver ions / 100 cm<sup>2</sup> in 24 h and was found to completely mitigate wound colonizers *S.aureus*, *P.aeruginosa*, *E.coli* and *Candida albicans*.<sup>19</sup> The effect of different degree of PVA hydrolysis on the silver ion release from PVA-AgNPs hydrogels and its anti-biofilm effect against *P.aeruginosa* and *S.aureus* have also been explored.<sup>20</sup> These studies clearly suggest that the surface ligands indeed play a significant role in increasing or modulating the antibacterial properties of AgNPs.

Natural phenolic compounds have displayed versatile biological properties encompassing antibacterial, antiviral, antifungal and anti-carcinogenic properties.<sup>21,22</sup> One striking example is the resistance of stilbenes, grape phenols, to fungal colonization.<sup>23</sup> Furthermore, the easy ionization properties of phenols have been successfully exploited for the synthesis of AgNPs.<sup>24</sup> The guest interacting properties of phenols have been exploited to fabricate surface functionalized AgNPs for selective colorimetric sensing of metal cations and anions in aqueous solution.<sup>25-28</sup> The phenolic molecules can act as reducing, stabilizing as well as surface functionalizing molecules. Herein, we report the unusual nano-assembly of AgNPs using 2-(2-hydroxybenzylamino)-4-(methylthio)butanoic acid (L), a methionine attached phenolic molecule as reducing agent together with capping molecules poly(styrene sulfonate) (PSS), poly(vinyl alcohol) (PVA), poly(vinyl pyrrolidone) (PVP) and sodium dodecylsulfate (SDS) that exhibited efficient growth inhibition of biofilm. The slow reduction of Ag<sup>+</sup> ions and thiophilic interaction of L lead to the formation of interesting nano-assembly of AgNPs such as flower petals and mesocrystals. Anti-biofilm studies of AgNPs were evaluated against four different bacteria viz., *S. aureus*, *P. aeruginosa*, *B. subtilis* and *E. coli* and efforts to discern mechanism of antibiofilm effect were undertaken. Based on our results, we propose that L-capping agents – AgNPs could be potentially employed in wound healing applications, to curtail biofilms formed by drug resistant bacteria.

### Experimental Section

Methionine, cysteine, ethanol and NaOH were obtained from Ranbaxy fine chemicals. Salicylaldehyde, NaBH<sub>4</sub>, AgNO<sub>3</sub>, poly(vinyl alcohol) (PVA, MWt 40,000), sodium salt of poly(styrene sulfonate) (PSS, MWt 40,000), sodium dodecylsulfate (SDS) and poly(vinyl pyrrolidone) (PVP, MWt 40,000) were obtained from Sigma-Aldrich. Mill-Q water was used for all the experiments.

#### SYNTHESIS OF 2-(2-HYDROXYBENZYLAMINO)-4-(METHYLTHIO)BUTANOIC ACID (1)

Reduced Schiff base phenolic chelating ligand (1) was synthesized by following the reported procedure.<sup>25</sup> Typically one equivalent of methionine was dissolved in 20 ml of water using 1:1 NaOH. To this solution, ethanol solution of

salicylaldehyde (1 equivalent, 10 ml) was added under vigorous stirring at room temperature. The solution has turned immediately bright yellow colour and the stirring was continued for another 30 min. Then the reaction mixture was cooled in ice-bath and NaBH<sub>4</sub> (1.5 equivalent) was added in portion-wise. The bright yellow colour was slowly disappeared and neutralization of the reaction mixture produced precipitates of 1. The precipitate was filtered, washed with cold ethanol and dried in vacuum.

1. Yield = 85 %. <sup>1</sup>H NMR (d<sub>6</sub>-DMSO) δ 7.14-7.25 (m, 2H), 6.75-6.84 (m, 2H), 3.85-3.99 (q, 2H), 3.25-3.29 (t, 1H), 2.50-2.65 (m, 2H), 2.02 (s, 3H), 1.85-1.95 (m, 2H). <sup>13</sup>C NMR (CDCl<sub>3</sub>) δ 171.11, 156.39, 130.39, 129.37, 120.94, 118.78, 115.46, 59.60, 46.41, 30.44, 29.75, 14.44. C<sub>12</sub>H<sub>17</sub>N<sub>3</sub>O<sub>3</sub> (255.33): calcd. C 56.45, H 6.71, N 5.49; found C 56.70, H 6.48, N 5.62. m/z (LC-MS) 256.00 (M+H).

#### SYNTHESIS OF 1-AGNPS WITH CAPPING AGENTS

Aqueous solution of 1 (0.1 M), AgNO<sub>3</sub> (0.1 M) and capping molecules (1 wt % for PSS, PVA and PVP whereas 0.5 M for SDS) were prepared separately. 1 was dissolved using 1:1 equivalent of NaOH. Then 5 ml of capping molecules and 5 ml AgNO<sub>3</sub> was mixed together. 5 ml of 1 was added to this mixture with stirring at room temperature. The resulting solution was stirred for 30 min and was allowed to stand at room temperature for three days. The colorless solution slowly turned to pink to reddish brown depend on the capping molecules that indicates the formation of AgNPs. The above concentration for 1, AgNO<sub>3</sub> and capping molecules were chosen after series experiments with different combinations. Increasing the concentration of AgNO<sub>3</sub> or 1 or reducing the concentration of capping molecules lead to settling down of AgNPs slowly. The AgNPs synthesized using PSS, PVA, PVP and SDS capping molecules are named as 1-PSS-, 1-PVA-, 1-PVP- and 1-SDS-AgNPs.

#### CHARACTERIZATION

The UV-visible measurements were performed using a Perkin Elmer model Lambda 1050, at the resolution of 1 nm. The size and morphology of AgNPs were investigated using High Resolution Transmission Electron Microscopy (HR-TEM, JEOL JEM-2100F). Samples for TEM measurements were prepared by placing a drop of NPs solution on the graphite grid and drying it in vacuum.

#### ANTIBACTERIAL STUDIES

Minimum inhibitory concentrations (MIC) and Minimum bactericidal concentration (MBC) for nanocomposites (1-PSS-AgNPs, 1-PVA-AgNPs, 1-PVP-AgNPs and 1-SDS-AgNPs) and various controls viz., 1, capping molecules (PSS, PVA, PVP and SDS) alone as well as 1 with capping molecules (1-PSS, 1-PVA, 1-PVP and 1-SDS) and silver nitrate was determined for representative gram positive (*S.aureus* and *B.subtilis*) and representative gram negative bacteria (*P.aeruginosa* and *E.coli*) as reported earlier.<sup>29</sup>

#### BIOFILM INHIBITION ASSAY

Inhibition of biofilm formation by 1, capping molecules (SDS, PVA, PVP and PSS) separately, 1 with capping molecules (1-PSS, 1-PVA, 1-PVP and 1-SDS) and nanocomposites (1-PSS-

AgNPs, 1-PVA-AgNPs, 1-PVP-AgNPs and 1-SDS-AgNPs) were determined and quantified by crystal violet staining as reported earlier.<sup>30</sup> Overnight grown cells of *Pseudomonas aeruginosa*, *E.coli* (Gram negative bacterium) and *Bacillus subtilis* and *Staphylococcus aureus* (Gram positive bacterium) were diluted (1:100) in sterile Tryptic soy broth and inoculated into micro titer plates containing increasing concentrations of polymeric nanomaterials as mentioned above in dilute (0.01X) Tryptic Soy Broth, after 18-24 h the micro titer plates were washed with PBS to remove unbound cells, dried and stained with 0.1% crystal violet for 15-20min. The plates were washed thoroughly in PBS and dried in an oven at 60°C. Crystal violet was extracted using 30% acetic acid for 15-20min and absorbance was recorded at 595nm using a microplate reader (BioRad, USA).

#### CONFOCAL IMAGING

Based on the differential anti-biofilm effect of PVP in combination with 1, we chose PVP and its different derivatives as treatments to visualize anti-biofilm effect by confocal imaging. Live dead staining followed by confocal imaging on biofilms with and without treatment by PVP and its derivatives were performed as reported earlier.<sup>31</sup> Briefly, biofilms formed on the surface of cover slips placed inside sterile six-well plates containing 0.1X TSB media. Every 18 h, spent media was replaced with fresh sterile media. For sampling, slides were removed on Day 2, washed with sterile PBS to remove the non-adherent cells and stained with a mixture of acridine orange (0.2mg/ml) and propidium iodide (0.33mg/ml) and imaged using Olympus FV 1000 confocal microscope with 63X objective, at a numerical aperture 0.3. For acridine orange, excitation was done using Multi Argon LASER and for detecting fluorescence due to propidium iodide, excitation was performed using Helium Neon LASER. Acridine orange stains the nucleic acids of live cells which when excited emits green fluorescence whereas, propidium iodide stains nucleic acids in membrane compromised or dead cells. Upon excitation, propidium iodide emits red fluorescence. Thus all viable cells would appear green and all dead cells would appear red.

#### 1-N-PHENYLNAPHTHYLAMINE (NPN)-ASSAY

Since 1 preferentially inhibits biofilms formed by gram negative bacterium, we investigated if the anti-biofilm effect of 1 could be due to altered outer membrane permeability. To assess the extent of outer membrane damage in *Pseudomonas aeruginosa* and *E.coli* (gram negative bacteria) caused by 1, we performed NPN based membrane permeability assay as reported earlier.<sup>32</sup> NPN exhibits enhanced fluorescence in phospholipid environment. Typically, Outer Membrane (OM) of gram negative bacteria prevents the access for hydrophobic molecules as it contains LPS, increased fluorescence indicates enhanced OM permeability. Briefly, cells were grown to mid-log phase collected and washed with 5mM HEPES buffer containing 0.2% glucose at pH 7.5 and resuspended in an equal volume of the same buffer. NPN was added at a concentration of 0.5 mM, this was immediately followed by addition of 1 in increasing concentrations. Fluorescence due to NPN was measured (Ex350 and Em 420 nm) and NPN uptake factor was

computed as reported earlier. Suitable controls were maintained.

#### MEMBRANE DEPolarization STUDIES

The ability of the reducing agent 1 to perturb membrane potential was discerned using the fluorophore DiSc<sub>3</sub> [3,3'-Dipropylthiadicarbocyanine iodide] as reported earlier.<sup>33</sup> DiSc<sub>3</sub> partitions to lipid bilayer if the membrane potential is unperturbed. When the membrane potential is perturbed, it partitions to the aqueous region wherein, its fluorescence is enhanced. Briefly, mid-log phase cells were pelleted, resuspended in 5mM HEPES buffer [2-[4-(2-hydroxyethyl)piperazin-1-yl]ethanesulfonic acid] and challenged with 1 at 0.5X MIC. After 30min of incubation, 2µl of DiSc<sub>3</sub> [3,3'-Dipropylthiadicarbocyanine iodide] was added and the readings recorded for 5min (Ex at 622nm and Em at 670nm). Protonophore CCCP was used as a positive control.

#### ROS ASSAY

To discern if 1 induced ROS production 2'-7'-dichlorofluorescein diacetate was used as a probe and endogeneous ROS production was measured spectrofluorimetrically by acquiring fluorescence intensity as reported earlier.<sup>34</sup> H<sub>2</sub>O<sub>2</sub> was used as a positive control. Fluorescence intensity was normalized with respect growth of each culture.

#### MOTILITY ASSAYS

Swimming, swarming and twitching motilities for *E.coli* and *P.aeruginosa* were performed exactly as reported earlier.<sup>35</sup>

## Results and Discussion

### SYNTHESIS AND CHARACTERIZATION OF 1 AND AgNPs

L, a methionine amino acid based phenolic molecule, was synthesized by Schiff base condensation of methionine with salicylaldehyde followed by imine reduction using NaBH<sub>4</sub>. We have been working with phenolic molecules as reducing, stabilizing and surface functionalizing agents of AgNPs for selective colorimetric sensing of metal cations and anions.<sup>26-28</sup> The easy ionization potential of phenolic functionality can reduce silver ions into AgNPs and chelating metal interacting functionality could stabilize the NPs. Noble metal nanoparticles such as Ag and AuNPs exhibit strong visible color due to surface plasmon resonance (SPR) vibration.<sup>36</sup> The linear lipophilic side chain of L along with sulphur group that can have preferential interactions with noble metal surface might be useful in controlling AgNPs morphology and enhancing biological effect. However, L that is expected to act as both reducing and functionalizing agent did not stabilize AgNPs for a long time. It produced only black precipitate (Fig. 1a). But addition of L into AgNO<sub>3</sub> in presence of capping molecules PSS, PVA, PVP and SDS slowly produced stable transparent colloidal AgNPs solution with different colors (Fig. 1a). It takes three days to produce AgNPs solution with stable color. L with other commonly used capping molecules such as polyethylene glycol (PEG), chitosan and tween-80 has also been studied but they also did not produce stable AgNPs. Absorption spectra of L-AgNPs did not show any characteristic peak since it precipitated-out and confirm that L alone is incapable to

## ARTICLE

## Journal Name

stabilize AgNPs. The orange pink solution of L-PSS-AgNPs showed absorption at 460 nm whereas L-PVA-AgNPs (reddish

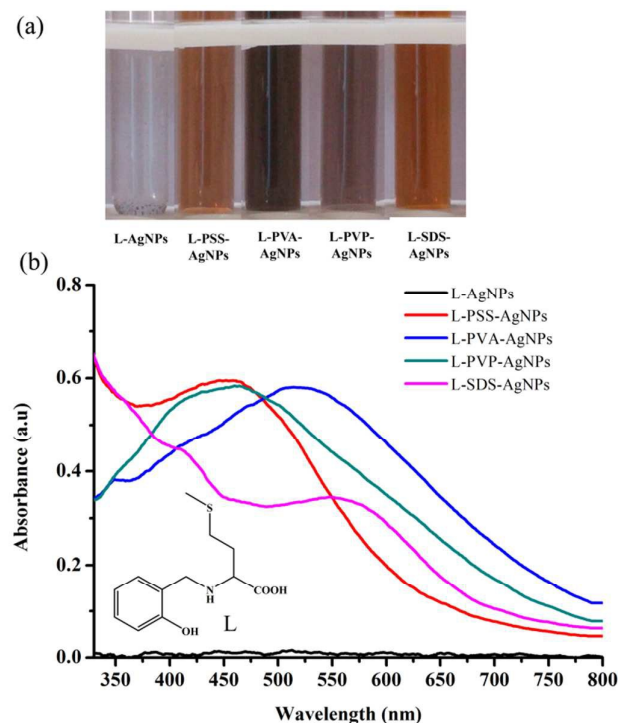
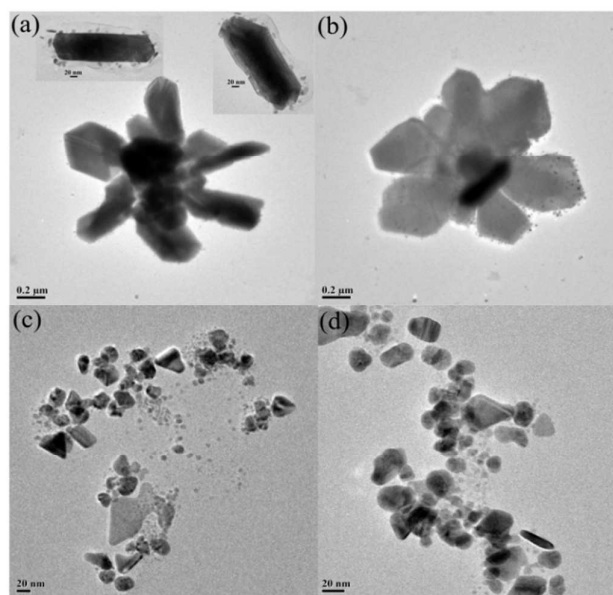


Fig. 1. (a) Digital images and (b) absorption spectra of AgNPs synthesized using L without and with different capping molecules (PSS, PVA, PVP and SDS).

brown) showed absorption at 518 nm (Fig. 1b). The pink L-PVP-AgNPs solution showed broad absorption spectrum with  $\lambda_{\max}$  at 465 nm. L-SDS-AgNPs also showed orange pink color and exhibited broad spectrum with two absorption peaks at 408 and 566 nm. This looks interesting since other amino acid (valine, isoleucine, leucine) attached phenolic molecules that produced stable AgNPs immediately without extra capping agents showed absorption between 395 to 420 nm.<sup>25,26</sup> Further, the presence of capping agents also did not alter the AgNPs absorption significantly. It is noted that AgNPs prepared using conventional sodium borohydride ( $\text{NaBH}_4$ ) reducing agents in presence of PSS, PVA, PVP and SDS capping molecules showed narrow absorption around 410 nm (Fig. S1). The appearance of different color, broad and longer wavelength absorption indicates the formation of polydispersed AgNPs with different morphology that was confirmed by HR-TEM studies (Fig. 2,3). Typical spherical AgNPs between 5 to 50 nm commonly show yellow color with absorption range between 390 - 440 nm.<sup>36</sup>

HR-TEM studies confirmed the formation of polydispersed AgNPs with different morphologies that further self-assembled into unusual nanostructures in presence of capping ligands. L-PSS-AgNPs revealed the formation of thin plates of AgNPs with length up to 400 nm and width between 100 - 300 nm (Fig. 2a,b). Interestingly, the thin plates self-assemble into micron sized flower petal structures in L-PSS-AgNPs. It is

noted that the formation of flower petal micro-structures has been observed over the whole sample (Fig. S2). The thin plates with clear edges form the petal morphologies (Fig. 2b, S2). L-PVA-AgNPs and L-PVP-AgNPs showed the formation of polydispersed AgNPs with diverse morphologies including triangular prisms, nanorods, spherical NPs and nanoplates (Fig. 2c,d, 3a,b, S3 and S4). TEM images of L-SDS-AgNPs showed the formation of nanospheres (200 to 300 nm), which in turn is comprised of a dense assembly of the primary Ag nanoplates, with recognizable voids and boundaries between the particles (Fig. 3c,d and S5). The individual AgNPs are likely to have length of 20 nm and a diameter of 5-10 nm. Thus, simple phenolic chelating ligand, L, in presence of capping agents reduces  $\text{Ag}^+$  ions into AgNPs with different morphologies preferentially nanoplates that further self-assemble into unusual



and unique nanostructures. This could be attributed to the slow Fig. 2. HR-TEM images of (a, b) L-PSS-AgNPs and (c, d) L-PVA-AgNPs. The inset in (a) shows the nanoplates of AgNPs.

evolution of AgNPs by weak reducing effect of (L) and competing preferential interaction of sulphur group of L with AgNPs. It is likely that the structure of nanocomposites could be further aided by the interaction of L- AgNPs with different stabilizing agent (PSS, PVA, PVP and SDS). It is noted that AgNPs synthesized using  $\text{NaBH}_4$  reducing agent produced yellow color instantaneously in presence of same four capping molecules and resulted in the formation of spherical AgNPs (Fig. S6). L alone without capping molecules failed to produce stable AgNPs and produced only black-grey precipitates. Furthermore, phenolic chelating ligands based on other amino acids such as alanine and valine has been shown by our group to produce only spherical AgNPs irrespective of whether AgNPs were made with or without capping molecules.<sup>25</sup> These result clearly indicate that sulphur atom in the phenolic ligand together with capping molecules plays significant role in producing interesting morphologies and unusual assemblies. It

is noted that sulphur atom is known to have strong interaction with noble metal surface such as Ag and Au. Previous studies have shown that thiol based capping molecules can be used for effective controlling of metal NPs size and morphology by make use of thiophilic interaction with noble metal surface.<sup>37,38</sup>

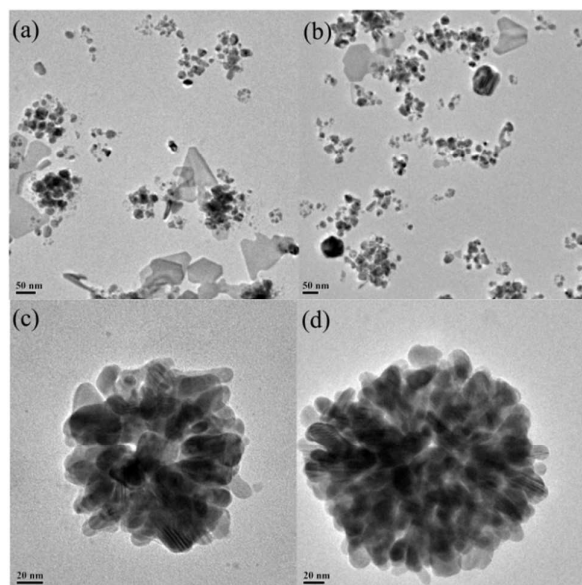


Fig. 3. HR-TEM images of (a, b) L-PVP-AgNPs and (c, d) L-SDS-AgNPs.

#### Antibacterial effect

We were interested to explore the effect of unusual morphology and enhanced lipophilic character of L on the antimicrobial activity of AgNPs. Minimum Inhibitory Concentration (MIC) and Minimum Bactericidal Concentration (MBC) studies were performed to evaluate the antimicrobial activity of AgNPs (Table 1).

L-AgNPs with all four capping molecules exhibited MIC in the range of 10 nM to 80 nM against three different bacteria (*P. aeruginosa*, *B. subtilis*, *S. aureus*) and with *E. coli*, MIC was higher by 2 fold (20 to 160 nM). When compared with NaBH<sub>4</sub> reduced AgNPs, L containing PSS and SDS AgNPs displayed an enhanced antibacterial effect against all 4 bacteria tested, probably due to its smaller size (nanoplates) and increased surface area (Figure 3). Whereas L-containing PVA and PVP AgNPs exhibited lower antibacterial effect, which could be attributed to their larger size (Figure 2). Although the reasons for increased MIC of L containing AgNPs against *E. coli* relative to other bacteria was not quite evident, our results discussed below reveal that L permeabilizes outer membrane of *E. coli* more efficiently than it does for *P. aeruginosa* (Table 3), thus L capped AgNPs are more likely to enter into *E. coli*. Despite increased outer membrane permeability decreased MIC probably indicates enhanced efflux of L containing AgNPs by *E. coli*.

Bactericidal studies (MBC) revealed that L-PSS-AgNPs exerted potent bactericidal effect from 20 to 40 nM. Whereas L-SDS-AgNPs required a two to four fold higher concentration to exert bactericidal effect. Both L-PVA- and L-PVP-AgNPs required much higher (~ 4 fold) concentration of AgNPs (80 to

160 nM) to exert bactericidal effect against all four bacteria tested. On the other hand, PVA and PVP capped AgNPs prepared using NaBH<sub>4</sub> were more effective in its bacteriostatic and bactericidal effect relative to SDS and PSS capped AgNPs (Table 1). SDS-AgNPs required 2-8 fold higher concentration relative to its L containing counterpart to show growth inhibition against the bacteria tested and in fact, PSS-AgNPs did not show any significant antimicrobial effect up to 160 nM tested. However, PVP and PVA capped AgNPs exhibited MIC and MBC at much lower concentration (2-8 folds lower) compared to L-PVP- and L-PVA-AgNPs.

Organism	<i>S. aureus</i>		<i>B. subtilis</i>		<i>P. aeruginosa</i>		<i>E. coli</i>	
	MIC (nM)	MBC (nM)	MIC (nM)	MBC (nM)	MIC (nM)	MBC (nM)	MIC (nM)	MBC (nM)
L-PSS-AgNPs	10	20	10	20	10	20	20	40
L-PVA-AgNPs	40	80	80	>160	40	80	80	>160
L-PVP-AgNPs	40	160	80	>160	80	>160	160	>160
L-SDS-AgNPs	10	40	20	40	40	80	40	80
PSS-AgNPs	>160	>160	>160	>160	>160	>160	>160	>160
PVA-AgNPs	10	20	10	20	20	40	20	40
PVP-AgNPs	20	40	20	40	20	40	20	40
SDS-AgNPs	80	160	80	160	160	>160	80	160

Table 1. Antibacterial effect of L-capping agent-AgNPs and capping agent-AgNPs synthesized using NaBH<sub>4</sub> without L.

The size, morphology and surface capping molecules of AgNPs are known to exert strong influence on the antimicrobial effect.<sup>17,39</sup> The capping molecules that provides higher stability shows weaker antimicrobial activity due to slow/no release of silver ions. Similarly smaller NPs or morphologies with higher surface area tend to exhibit enhanced antimicrobial effects. Hence strongly stabilized spherical PSS- and SDS-AgNPs without L exhibited lowest antimicrobial activity. However, L-PSS- and L-SDS-AgNPs, which

## ARTICLE

## Journal Name

showed the formation of nano plates of AgNPs that were further self-assembled into micron/nano sized flower petals and mesocrystals, displayed enhanced antimicrobial effect. Our observations imply that the formation of plate morphologies with higher surface area and self-assembly of nanoplates into micro/bigger nano-structures resulted in enhanced antimicrobial activity. PVA- and PVP-AgNPs displayed more potent antimicrobial effect relative to L-PVA- and L-PVP-AgNPs, despite forming poly dispersed nanostructures with altogether different morphology. An earlier study showed that  $\text{NaBH}_4$  reduced AgNPs capped with PVP displayed synergy with antibiotics and mitigated both gram positive and gram negative bacteria effectively relative to citrate and SDS capped AgNPs.<sup>39</sup> In this study, synergy could not be discerned by checkerboard method since L and most of the capping molecules tested did not display any anti-bacterial effect. Previous report showed that plant extract reduced CTAB capped AgNPs displayed enhanced antibacterial effect against methicillin resistant *Staphylococcus aureus* (MRSA) relative to SDS stabilized AgNPs.<sup>40</sup> It was also shown that PSS-Ag nanocomposite exhibited good mobility of AgNPs and exerted antibacterial effect against *S. aureus* and *S. epidermidis* at higher concentration range (500  $\mu\text{g}/\text{ml}$  to 2000  $\mu\text{g}/\text{ml}$ ) depending upon the bacterial inoculum density.<sup>41</sup> Thus polymers with varying stabilizing effect elicits differential release of silver ions, which in turn affects the observed MIC and MBC values. Overall among all AgNPs evaluated, L-PSS-AgNPs was most effective at a lower concentration against all four bacteria tested and in fact a strong antibacterial effect against both *S. aureus* and *P. aeruginosa*, which are tough to eradicate was exhibited by L-PSS-AgNPs at a much lower concentration of 10-20 nM, implying good enhancement in the antibacterial effect of AgNPs when L was used as a reducing and functionalizing agent.

#### Anti-biofilm studies

The enhanced antibacterial effect of AgNPs when prepared using L and synergistic effect if any of phenolic structure with capping molecules prompted us to explore its anti-biofilm activity. Crystal violet assay is a good indicator of biofilm biomass. We evaluated the ability of L-PSS-, L-PVA-, L-PVP- and L-SDS-AgNPs to prevent biofilm formation in two gram positive bacteria (*B. subtilis* and *S. aureus*) and two gram negative bacteria (*P. aeruginosa* and *E. coli*). Various controls like PSS-, PVA-, PVP- and SDS-AgNPs prepared using  $\text{NaBH}_4$  as the reducing agent, capping molecules alone, reducing agent (L) alone and L with capping molecules were employed.

Our results indicate that L-PSS-, L-PVA-, L-PVP and L-SDS-AgNPs exhibited significantly stronger anti-biofilm effect relative to AgNPs prepared using sodium borohydride as reducing agent (Fig. 4). Untreated biofilms were used as control. Among AgNPs with L, SDS and PSS capped AgNPs were most effective at lowest concentration of 10 nM followed by PVA and PVP capped AgNPs, which exerted their anti-biofilm effect at 20 nM (Fig. 4a-d). However, among AgNPs using  $\text{NaBH}_4$ , only PVP capped AgNPs displayed anti-biofilm effect in the range of 20 to 40 nM, followed by SDS capped AgNPs,

which was effective at 80 nM (Fig. 4e-h). It is likely that among AgNPs without L, PVP-AgNPs release more Ag ions, which could probably account for enhanced antibiofilm effect. PSS- and PVA-AgNPs without L failed to induce discernible anti-biofilm effect in the entire concentration range tested. Furthermore, we observed that L-PSS-AgNPs were quite effective as an anti-biofilm agent against all four bacteria tested, whereas PSS-AgNPs without L did not exhibit any anti-biofilm effect. Hence it is plausible that the anti-biofilm effect of PSS-AgNPs could be mediated by L. The strong anti-biofilm activity of L-PSS-AgNPs could be of potential value in wound healing applications. It has been shown in an earlier work that PSS can favour osseointegration of artificial ligaments with bone tunnels, which is likely to result in enhanced healing following a surgical reconstruction.<sup>42</sup>

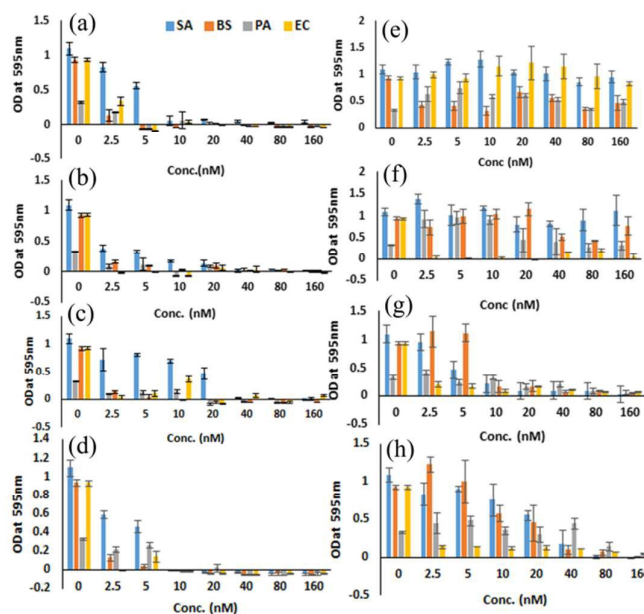


Fig. 4. Antibiofilm studies of (a) L-PSS-AgNPs, (b) L-PVA-AgNPs, (c) L-PVP-AgNPs, (d) L-SDS-AgNPs, (e) PSS-AgNPs, (f) PVA-AgNPs, (g) PVP-AgNPs and (h) SDS-AgNPs. SA = *Staphylococcus aureus*, BS = *Bacillus subtilis*, PA = *Pseudomonas aeruginosa* and EC = *E. coli*.

Comparing BIC (Biofilm inhibitory concentration) with MIC would reveal whether antibiofilm effect of L-capping agent-AgNPs arises due to antibacterial effect or they exhibit true antibiofilm effect. We observed that BIC of L-PSS-, L-PVA-, L-PVP- and L-SDS-AgNPs was lower than its MIC by 2-16 fold in *S. aureus*, with rest of the bacteria, BIC of nanomaterials were 2-64 fold lower than the corresponding MIC, implying that L-AgNPs with capping molecules exerted a true anti-biofilm effect, which is independent of its anti-bacterial effect (Table 2). On comparison of BIC of AgNPs with and without L, in case of *S. aureus*, *P. aeruginosa* and *B. subtilis*, AgNPs with L displayed 4-32 fold lower BIC relative to AgNPs without L. But with *E. coli*, BIC of PVA, PVP and SDS capped AgNPs with and without L matched with each other. Among capping agents only PSS capped AgNPs without L displayed a much higher BIC for all 4 microorganisms tested. Overall our results imply that AgNPs along with L and capping molecules exert lower BIC and

potent anti-biofilm effect against all 4 bacteria evaluated and by virtue of exhibiting true antibiofilm effect, L containing AgNPs can be effectively employed as a dressing material to

Organism	<i>S.aureus</i>		<i>B.subtilis</i>		<i>P.aeruginosa</i>		<i>E.coli</i>	
	MIC(nM)	BIC(nM)	MIC(nM)	BIC(nM)	MIC(nM)	BIC(nM)	MIC(nM)	BIC(nM)
L-PSS-AgNPs	10	10	10	2.5	10	5	20	5
L-PVA-AgNPs	40	2.5	80	2.5	40	2.5	80	2.5
L-PVP-AgNPs	40	20	80	2.5	80	2.5	160	2.5
L-SDS-AgNPs	10	5	20	2.5	40	10	40	5
PSS-AgNPs	>160	>160	>160	2.5	>160	>160	>160	>160
PVA-AgNPs	10	>160	10	80	20	80	20	2.5
PVP-AgNPs	20	5	20	10	20	20	20	2.5
SDS-AgNPs	80	20	80	20	160	80	80	2.5

curtail biofilm formation on wounds.

Table 2. Antibiofilm effects of L-capping agent-AgNPs and capping agent-AgNPs synthesized using NaBH<sub>4</sub> without L.

Reports on the anti-biofilm effect of silver from AgNPs against diverse bacteria including clinically relevant *P. aeruginosa* and *S. aureus* are prevalent.<sup>43-46</sup> In all these cases the anti-biofilm effect is predominantly due to the released silver ions, which acted as a bacteriostatic/ bactericidal agent. Surprisingly, we observed that with L-PSS-, L-PVA-, L-PVP- and L-SDS-AgNPs, BIC is much lesser than its corresponding MIC, implying anti-biofilm effect is not due to released Ag ions but could be attributed to the capping molecules, methionine based phenolic chelating ligand (L) or combination of both. Hence, we explored the anti-biofilm roles of individual components that make up the nanocomposite viz., L, capping molecules and L with capping molecules, against the four representative bacteria reported in this study.

As we observed a differential anti-biofilm effect between PSS-, PVA-, PVP- and SDS-AgNPs with and without L, the role of L in exerting anti-biofilm effect was explored. Interestingly at a concentration of 160 nM, L completely mitigated biofilm

formation by gram negative bacteria. Even at higher dilutions, significant biofilm inhibitory effect of L on gram negative bacteria was observed; however, L was unable to exert potent anti-biofilm effect against gram positive bacteria in the entire concentration range tested (Fig. 5). Whereas L-PSS-, L-PVA-, L-PVP- and L-SDS-AgNPs exerted anti-biofilm effect against both gram positive and gram negative bacteria at a much lower concentration independent of AgNPs' antibacterial effect (Fig. 4a-). This differential effect between L and L-capping molecule -AgNPs prompted us to evaluate a combination of L with capping molecules but without AgNPs so as to understand the synergistic effect or modulation of antibiofilm effect of L by the capping molecule(s). Towards this end, anti-

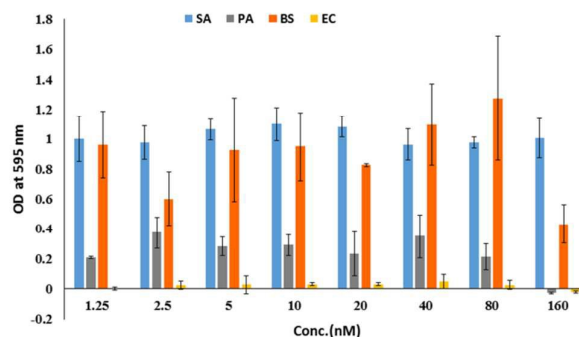


Fig. 5. Antibiofilm studies of L against gram positive and gram negative bacteria. SA = *Staphylococcus aureus*, BS = *Bacillus subtilis*, PA = *Pseudomonas aeruginosa* and EC = *E. coli*.

biofilm effect of L in combination with capping molecules was evaluated and capping molecules alone were used as controls. When polymers were tested alone, SDS exerted anti-biofilm effect against all four bacteria. PVP inhibited *E. coli* biofilms alone, whereas PSS caused a significant but not a drastic inhibition of biofilms formed by *E. coli* and *P. aeruginosa*. Quite unexpectedly, PVA alone at the highest concentration tested inhibited biofilms formed by all four bacteria (Fig. S7). Previous study has shown that SDS can hinder and even disperse mature biofilms when it was used in combination with sodium bicarbonate and sodium metaperiodate.<sup>47</sup> SDS loaded nanoporous polymer was also shown to block bacterial attachment in short term and prevent biofilm formation in long term.<sup>48</sup> SDS due to its anionic and amphipathic nature could possibly disrupt bacterial communication through pili<sup>49</sup> and nanotubes<sup>50</sup> and thereby prevent attachment and aggregation, which are prerequisites for biofilm formation.<sup>48</sup> PSS also exerted broad spectrum antimicrobial effect against STD pathogens *Chlamydia trachomatis* and *Neisseria gonorrhoeae*.<sup>51</sup> A biopolymer isolated from marine sponge has shown to exert anti-adhesive effect against *V. alginolyticus*, *V. harvei* and *V. parahaemolyticus*. Similarly, chitosan was found to hinder adherence, biofilm formation and interfere with mature biofilms in *S. mutans* compared to commercially available mouth washes.<sup>52-54</sup> Based on these studies, it is evident that polymers do exhibit anti-biofilm effect. The anti-biofilm effect of PVA against all four bacteria is a hitherto unreported interesting observation and the detailed mechanism bio-film

growth inhibition would be explored in future studies separately.

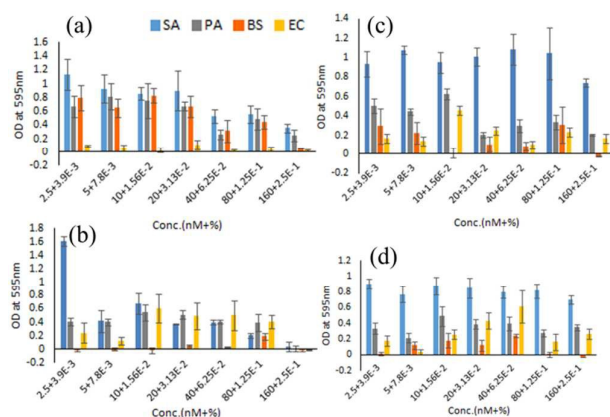


Fig. 6. Antibiofilm studies of (a) L-PSS, (b) L-PVP, (c) L-PVA and (d) L-SDS compositions. SA = *Staphylococcus aureus*, BS = *Bacillus subtilis*, PA = *Pseudomonas aeruginosa* and EC = *E. coli*. X axis label Conc. (nM +%) signifies concentration of ligand (L) in nM in combination with the concentration of the polymer in %.

Among the combination of L with PSS, PVA, PVP and SDS capping molecules, only L-PVP exerted anti-biofilm effect against all the four bacteria tested (Fig. 6). PVP alone did not display significant anti-biofilm effect (Fig. S7) and L was effective only against gram negative bacteria. The phenolic ligand L in combination with PVP was able to effectively inhibit biofilms formed by all four bacteria (Fig 6). So it is evident that L in combination with PVP modulates anti-biofilm activity of PVP. Whereas when used in combination with other three capping molecules (PVA, PSS and SDS), L could not retain its anti-biofilm effect against *P. aeruginosa*. In fact L-PSS inhibited only *E. coli* and L-SDS and L-PVA lost their biofilm inhibitory effect against both *P. aeruginosa* and *E. coli*, but was effective against *B. subtilis*. Thus, our results imply that among capping agents, SDS and PVA alone at higher concentration and among combination of L with capping agents L-PVP at slightly higher concentrations and from L -capping agent – AgNPs, L-PSS- and L-SDS-AgNPs at lower concentrations were effective in preventing biofilm formation by all four bacteria tested. Although polymer alone and polymer in combination with L itself displayed effective antibiofilm effect albeit at higher concentration, L containing polymer capped AgNPs were made because, AgNPs have been shown in many earlier studies to heal chronic wounds and polymer capped AgNPs that release Ag in a sustained manner have been proven as a good wound dressing material.<sup>55</sup> This is supported by the earlier report which showed that biological dressings usually lead to wound deepening and chronic wound formation in burn wounds, which can be abrogated by impregnating dressing materials with AgNPs.<sup>21</sup>

In order to understand whether the observed anti-biofilm effect was due to reduced viability or impaired colonization, we performed confocal live/dead imaging of a representative L-AgNPs with appropriate controls. L-PVP-AgNPs was chosen for confocal imaging because among L and capping molecules

combinations, only L-PVP displayed anti-biofilm effect against all four bacteria tested. In addition, PVP-AgNPs without L also displayed anti-biofilm effect against all bacteria albeit at higher concentrations. Hence, the confocal live dead imaging of biofilms formed by *P. aeruginosa* and *S. aureus* (classical colonizers in wounds), were performed subsequent to the following treatments viz., PVP alone, L-PVP combination, L-PVP-AgNP. PVP-AgNPs with NaBH<sub>4</sub> and AgNO<sub>3</sub> solutions were used as controls. For treatment with L alone, live dead staining was performed only with gram negative bacteria since L was effective only against gram negative bacteria hence, despite being effective, its utility as a potential wound dressing material is limited, because wounds are typically colonized by polymicrobial communities comprised of both gram positive and gram negative bacteria, which inevitably forms biofilms and thus we evaluated the antibiofilm effect of L along with capping molecule and AgNPs.

*P. aeruginosa* and *S. aureus* are classical colonizers of chronic/burn wounds. With *P. aeruginosa*, treatment by L alone, L-PVP and L-PVP-AgNPs resulted in impaired colonization (Fig. 7). In contrast, treatment with controls, PVP-AgNPs and AgNO<sub>3</sub>, caused increased proportion of dead cells, which contributed to its anti-biofilm effect (Fig. S8, S9). Similarly, L, L-PVP and L-PVP-AgNPs caused impaired colonization with *S. aureus*, whereas PVP-AgNPs and AgNO<sub>3</sub> exhibited enhanced killing, probably due to the released silver ions (Fig. 8). Hence, the results from confocal imaging broadly shows that with *P. aeruginosa* and *S. aureus*, the anti-biofilm effect of individual components that make up the NPs and the

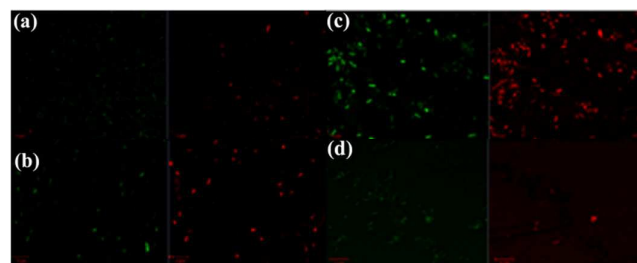


Fig. 7. Live-dead staining and confocal imaging of *P. aeruginosa* treated with (a) L, (b) PVP, (c) L-PVP and (d) L-PVP-AgNPs. *P. aeruginosa* was grown for 3 days on the surface of a glass slide in 0.1 X nutrient broth and tryptic soy broth respectively, stained with acridine orange and propidium iodide and imaged using confocal microscopy.

L-PVP-AgNPs can be predominantly attributed to impaired colonization, which correlates well with the observation of BIC < MIC and also with the fact that the anti-biofilm effect of L-PSS-, L-PVA-, L-PVP- and L-SDS-AgNPs is true anti-biofilm effect, which is independent of its antibacterial effect due to released silver ions.

#### Mechanism of action of L

In order to gain insight on the mechanism of anti-biofilm effect exerted by L, different studies such as membrane permeability, membrane potential, membrane integrity, ROS generation and motility assays were performed.

NPN was used to assess membrane permeability. NPN shows enhanced fluorescence in lipid environment compared to aqueous environment. If the test compound affects

membrane permeability, NPN will partition to lipid environment resulting in enhanced fluorescence. Since L caused anti-biofilm effect exclusively against gram negative bacteria, the effect of L on the outer membrane (OM) permeability in gram negative bacteria was explored. The results showed that treatment with L induced a significant increase in NPN uptake factor of 7.8 for *P. aeruginosa* and 8.77 for *E. coli* (Table S1). A high NPN uptake factor implies that the OM of gram negative bacteria is permeabilized by L. Thus the observed decreased colonization of bacteria especially with *P. aeruginosa* in confocal imaging by L could be due to the increased permeability that might interfere with intracellular accumulation of quorum sensing (QS) molecule, thereby hindering biofilm formation. A recent study has shown that myco-fabricated AgNPs inhibited quorum sensing, secretion of virulence factors and biofilm formation in *P. aeruginosa*.<sup>56</sup>

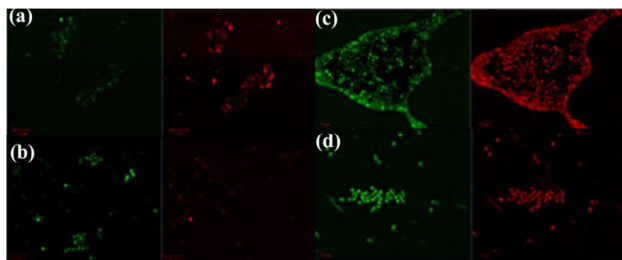


Fig.8. Live-dead staining and confocal imaging of *S. aureus* treated with (a) L, (b) PVP, (c) L-PVP and (d) L-PVP-AgNPs. *S. aureus* was grown for 3 days on the surface of a glass slide in 0.1 X nutrient broth and tryptic soy broth respectively, stained with acridine orange and propidium iodide and imaged using confocal microscopy.

Membrane integrity was evaluated by quantifying release of protein (A280) and release of nucleic acids (A260) due to treatment with L and Triton X 100 (positive control), untreated bacterial cells were used as control. Relative to untreated *E. coli* cells, significant protein leakage (A280 of 0.368 Vs 0.819) was observed in L treated cells, which was equivalent to  $\sim 1/2$  of protein released due to treatment with Triton X 100 (A280 of 1.815). *P. aeruginosa* also showed a similar trend with L causing increased protein leakage relative to untreated cells (A280 of 0.304 vs 0.709), whereas Triton X 100 treatment caused  $\sim 3$  fold increase in protein release (A280 of 1.994). Even with nucleic acids, significant leakage was observed due to L treatment in both *E. coli* (A260 of untreated 0.34; 1 treated 0.54; Triton X treated 1.94) and *P. aeruginosa* (A260 of untreated 0.348; 1 treated 0.509 and Triton X 100 treated 1.203). Thus it is likely that L exerts its anti-biofilm effect in gram negative bacteria by altering membrane permeability which concomitantly results in leakage of protein and nucleic acid from the bacterial cells.

The ability of L to induce endogenous ROS production in all four bacteria were explored by 2',7' dichlorofluorescein diacetate (DCFH-DA) method as reported earlier.<sup>34</sup> 2',7' dichlorofluorescein (DCFH) is considered as a good indicator of overall oxidative status of the cell.<sup>57</sup> Hydrophobic non fluorescent DCFH-DA penetrates into the cell where it is cleaved by esterases and oxidized by cellular ROS to fluorescent 2,7-dichlorofluorescein (DCF) that can be

quantified by spectrofluorimetry. Our observations showed that only in case of *P. aeruginosa*, L caused 50% increase in endogenous ROS relative to untreated cells, which was incidentally 50 % lower than ROS formed due to treatment with hydrogen peroxide. Interestingly the fluorescence obtained in *P. aeruginosa* with hydrogen peroxide treatment was much lower compared to other cells, even though the reasons are unclear, fluorescence quenching/protection against oxidative stress by bacterial pigments might be responsible for this observation. An earlier study has shown that Staphyloxanthin protects *S. aureus* against oxidative stress.<sup>57</sup> In all other cases L did not cause any difference in ROS production relative to untreated cells and in fact it appeared that L quenched ROS production in *E. coli*, *B. subtilis* and *S. aureus*. Membrane potential remained unperturbed due to L treatment and motility also remained unaffected due to L treatment (data not shown) revealing that altered membrane permeability and membrane integrity is likely to account for anti-biofilm effect of L.

## Conclusion

Bacterial biofilms serve as a source of recurrent/ persistent infections particularly with respect to infections on chronic wounds and biofilms formed on implantable medical devices. Due to multifarious factors like EPS, heterogeneity, degradation, sequestration, slow growth phenotype etc., biofilms display antimicrobial resistance and are highly recalcitrant. By their mere presence and secretion of virulence factors, biofilms trigger a persistent inflammatory response, which significantly impairs wound healing. As biofilms are tough to eradicate, constant demand for non-toxic biomaterials as wound dressing materials with good anti-biofilm properties continues unabated. Our study showed that methionine phenolic chelating ligand (L) produced nanoplates of AgNPs with unusual assembly of nanostructures that resulted in the strong enhancement of anti-biofilm activity of polymer capped AgNPs. The effective inhibition of biofilms at lower concentration (BIC, Biofilm inhibitory concentration) compared to antimicrobial activity (MIC, Minimum inhibitory concentration) suggested the true anti-biofilm effect displayed by L-capping agent-AgNPs. Furthermore, L-PVP-AgNPs also exhibited stronger biofilm inhibitory effect against all four bacteria relative to the individual components as well as AgNPs without L. Studies to unravel the mechanism of action indicate that the increased anti-biofilm activity of L-AgNPs-capping agents could be due to altered membrane permeability and integrity caused by L. Thus a simple amino acid based phenolic chelating ligand led to usual assembly AgNPs and resulted in enhanced anti-biofilm activity which could be potentially exploited as a wound dressing material for wound healing applications.

## Acknowledgement

## ARTICLE

## Journal Name

Financial support from the Department of Science and Technology, New Delhi, India (DST Fast Track scheme no. SR/FT/CS-03/2011(G) and DST–FIST Grant no: SR/FST/ETI-331/2013) is acknowledged with gratitude. We thank CRF, SASTRA University for providing infrastructural support in the form of UV-Visible spectrophotometer.

## Notes and references

- M. C. Daniel and D. Astruc, *Chem. Rev.* 2004, **104**, 293–346.
- R. Mout, D. F. Moyano, S. Rana and V. M. Rotello, *Chem. Soc. Rev.* 2012, **41**, 2539–2544.
- O. N. Oliveira, R. M. Lost, J. R. Siqueira, F. N. Crespillo and L. Caseli, *ACS Appl. Mater. Interfaces* 2014, **6**, 14745–14766.
- Antibiotic resistance threats in the United States, 2013. Atlanta, GA: US Department of Health and Human Services, Washington, 2013. Available at <http://www.cdc.gov/drugresistance/threat-report-2013/>.
- B. Spellberg, R. Guidos, D. Gilbert, J. Bradley, H. W. Boucher, W. M. Scheid, J. G. Bartlett and J. E. Edwards, *Clin. Infect. Dis.* 2008, **46**, 155–164.
- W. M. Dunne, *Clin. Microbiol. Rev.* 2002, **15**, 155–166.
- U. –C. Hipler, P. Elsner and J. Fluhr, *Curr Probl Dermatol.*, Basel, Karger. 2006, **33**, 144–151.
- A. D. Russell and W. B. Hugo, *Prog Med Chem.* 1994, **31**, 351–370.
- H. Y. Lee, H. K. Park, Y. M. Lee, K. Kim and S. B. Park, *Chem Commun.* 2007, **28**, 2959–2961.
- V. Alt, T. Bechert, P. Steinrücke, M. Wagener, P. Seidel and E. Dingeldein, *Biomaterials* 2004, **25**, 4383–4391.
- X. Chen and H. J. Schluesener, *Toxicol. Lett.* 2008, **176**, 1–12.
- A. M. C. Ribeiro and L. D. M. Carrasco, *Int. J. Mol. Sci.* 2013, **14**, 9906–9946.
- V. V. Kumar, S. Anbarasan, L. R. Christena, N. SaiSubramanian and S. P. Anthony, *Spectrochimica Acta Part A: Molecular and Biomolecular Spectroscopy* 2014, **129**, 35–42.
- S. Kittler, C. Greulich, J. Diendorf, M. Koller and M. Epple, *Chem. Mater.* 2010, **22**, 4548–4554.
- M. Liong, B. France, K. A. Bradley and J. I. Zink, *Adv. Mater.* 2009, **21**, 1684–1689.
- X. Li, S. M. Robinson, A. Gupta, K. Saha, Z. Jiang, D. F. Moyano, A. Sahar, M. A. Riley and V. M. Rotello, *ACS Nano*, 2014, **8**, 10682–10686.
- X. Li, Y. –C. Yeh, K. Giri, R. Mout, R. F. Landis, Y. S. Prakash and V. M. Rotello, *Chem. Commun.* 2015, **51**, 282–285.
- L. Mei, Z. Lu, X. Zhang, C. Li and Y. Jia, *ACS Appl. Mater. Interfaces* 2014, **6**, 15813–15821.
- Z. Pei, Q. Sun, X. Sun, Y. Wang and P. Zhao, *Biomed Mater Eng.* 2015, **26**, (s1):S111–S118.
- D. Singh, A. Singh and R. Singh, *J Biomater Sci Polym Ed.* 2015, **26**, 1269–1285.
- M. M. Cowan, *Clin Microbiol Rev.* 1999, **12**, 564–582.
- R. P. Pimia, L. Nohynek, C. Meier, M. Kahkonen, M. Heinonen, A. Hopia and K. –M. O. Caldentey, *J Appl Microbiol.* 2001, **90**, 494–507.
- R. Hain, H. –J. Reif, E. Krause, R. Langebartels, H. Kindal, H.; Vornam, W. Wiese, E. Schmelzer, P. H. Schreier, R. H. Stocker and K. Stenzel, *Nature* 1993, **361**, 153–156.
- J. A. Jacob, H. S. Mahal, N. Biswas, T. Mukherjee and S. Kapoor, *Langmuir* 2008, **24**, 528–533.
- V. V. Kumar and S. P. Anthony, Silver nanoparticles based Sensors and Actuators B: Chemical 2014, **191**, 31–36.
- V. V. Kumar and S. P. Anthony, *RSC Adv.* 2014, **4**, 64717–64724.
- V. V. Kumar and S. P. Anthony, *New J. Chem.* 2015, **39**, 1308–1314.
- J. M. Andrews, *J Antimicrob Chemother* 2001, **48**, 5–16.
- J. H. Merritt, D. E. Kadouri and G. A. O'Toole, *Current Protocols in Microbiology* 2005, **1B**, 1, 1–17.
- H. Magesh, A. Kumar, A. Alam, Priyam, U. Sekar, V. N. Sumantran and Vaidyanathan, *Indian J Exp Biol.* 2013, **51**, 764–772.
- L. R. Christena, S. Subramaniam, M. Vidhyalakshmi, V. Mahadevan, A. Sivasubramanian and S. Nagarajan, *RSC Adv.* 2015, **5**, 61881–61887.
- I. M. Helander and T. M. Sandholm, *J Appl Microbiol.* 2000, **88**, 213–219.
- J. A. Silverman, N. G. Perlmutter and H. M. Shapiro, *Antimicrob Agents Chemother* 2003, **47**, 2538–2544.
- A. F. Tavares, M. Teixeira, C. C. Romao, J. D. Seixas, L. S. Nobre and L. M. Saraiva, *J Biol Chem.* 2011, **286**, 26708–26717.
- S. Chow, K. Gu, L. Jiang and A. Nassour, *Journal of Experimental Microbiology and Immunology* 2011, **15**, 22–29.
- P. Mulvaney, *Langmuir* 1996, **12**, 788–800.
- B. L. V. Prasad, S. I. Stoeva, C. M. Sorensen and K. J. Klabunde, K. J. *Langmuir* 2002, **18**, 7515–7520.
- S. D. Sidhaye and B. L. V. Prasad, *Chem. Mater.* 2010, **22**, 1680–1685.
- H. Jang, S. H. Lim, J. S. Choi and Y. Park, *Arch Pharm Res.* 2015, **38**, 1906–12.
- J. Girarda, P. S. Brunetto, O. Braissant, Z. Rajacic, N. Khannac, R. Landmann, A. U. Daniels and K. M. Fromma, *Comptes Rendus Chimie* 2013, **16**, 550–556.
- C. Vaquette, V. Viateau, S. Guerard, F. Anagnostou, M. Manassero, D. G. Castner and V. Migonney, *Biomaterials* 2013, **34**, 7048–7063.
- A. J. Kora and R. B. Sashidhar, *J Antibiot (Tokyo)* 2015, **68**, 88–97.
- N. K. Palanisamy, N. Ferina, A. N. Amirulhusni, Z. Mohd-Zain, J. Hussaini, L. J. Ping and R. Durairaj, *J. Nanobiotechnology*, 2014, **12**, 1–7.
- C. Y. Flores, A. G. Minan, C. A. Grillo, R. C. Salvarezza, C. Vericat and P. L. Schilardi, *ACS Appl Mater Interfaces*, 2013, **5**, 3149–3159.
- S. A. Masurkar, P. R. Chaudhari, V. B. Shidore and S. P. Kamble, *IET Nanobiotechnol*, 2012, **6**, 110–114.
- P. V. Gawande, K. LoVetri, N. Yakandawala, T. Romeo, G. G. Zhanel, D. G. Cvitkovitch and S. Madhyastha, *J. Appl. Microbiol.* 2008, **105**, 986–992.
- L. Li, S. Molin, L. Yang and S. Ndoni, *Int J Mol Sci.* 2013, **14**, 3050–3064.
- M. Achtman, G. Morelli and S. Schwuchow, *J. Bacteriol.* 1978, **135**, 1053–1061.
- G. P. Dubey and S. Ben-Yehuda, *Cell* 2011, **144**, 590–600.
- B. C. Herold, N. Bourne, D. Marcellino, R. Kirkpatrick, D. M. Strauss, L. J. Zaneveld, D. P. Waller, R. A. Anderson, C. J. Chany and B. J. Barham, *J Infect Dis.* 2000, **181**, 770–773.
- G. S. Kiran, A. N. Lipton, S. Priyadharshini, K. Anitha, L. E. Suarez, M. V. Arasu, K. C. Choi, J. Selvin and N. A. Al-Dhabi, *Microb Cell Fact.* 2014, **13**, 114 (1–12).
- E. M. Costa, S. Silva, A. R. Madureira, A. Cardelle-Cobas, F. K. Tavaría and M. M. Pintado, *Carbohydr Polym.* 2014, **101**, 1081–1086.
- E. M. Costa, S. Silva, F. K. Tavaría and M. M. Pintado, *Anaerobe* 2013, **20**, 27–31.
- M. Mohiti-Asli, B. Pourdeyhimi and E. G. Lobo, *Tissue Eng Part C Methods.* 2014, **20**, 790–797.
- B. R. Singh, B. N. Singh, A. Singh, W. Khan, A. H. Naqvi and H. B. Singh, *Sci. Rep.* 2015, **5**, 13719 (1–14).
- H. Wang and H. A. Joseph, *Free Radic Biol Med.* 1999, **27**, 612–616.

## Journal Name

## ARTICLE

57 A. Clauditz, A. Resch, K. P. Wieland, A. Peschel and F. Gotz,  
*Infect Immun.* 2006, **74**, 4950-4953.

## L-Methionine Based Phenolic Compound Mediate unusual Assembly of AgNPs and Exert Efficient anti-biofilm effect

Methionine based phenolic chelating ligand together with PSS, PVA, PVP and SDS capping agents produced unusual self-assembly of AgNPs and strong anti-biofilm effect against four different bacteria including S.aureus and P.aeruginosa, which are classical colonizers in burn wounds, in presence of PSS, PVA, PVP and SDS capping agents.

